ROMANIAN JOURNAL OF INFORMATION SCIENCE AND TECHNOLOGY
Volume **10**, Number 1, 2007, 53–66

A Comparative Study of Microcrystalline and Nanocrystalline Lead Sulfide Based $PbS/SiO_2/Si$ Heterostructures

V. STANCU, E. PENTIA, A. GOLDENBLUM,
M. BUDA, G. IORDACHE, T. BOTILA

National Institute of Material Physics
105 bis Atomiştilor St., Bucharest-Măgurele,
P.O. Box MG7, 77125, Romania
E-mail: mbuda@infim.ro

Abstract. The PbS micro-crystalline and nano-crystalline films were obtained using the Chemical Bath Deposition method. We investigated comparatively the structural, electrical and photoconductive properties of these films deposited on glass. $PbS/SiO_2/Si$ heterostructures made with nanocrystalline PbS layers present interesting peculiarities. Their C–V curves show hysterezis. In a field effect arrangement it is possible to control the photoconductive short and long wavelength ratio response. The heterostructure properties were explained by taking into account the interface charged traps.

Keywords: Optoelectronics, Nano-crystalline PbS, Heterostructures.

1. Introduction

PbS is an important A_4B_6 semiconductor with very good photoconductive properties in the infrared wavelength range (800–3 000 nm at room temperature). This range can be extended by combining PbS with Silicon in a heterostructure [1]. Recently [2, 3] the use of Si, Ge or metals in the nano-crystalline form was proposed for use in new types of DRAM or FLASH memories. In this paper we present a more complex heterostructure: $PbS/SiO_2/Si$ based on nanocrystalline PbS The properties of heterostructures of the nano-crystalline PbS deposited on p-Si/SiO_2 were not yet studied.

The PbS is deposited usually as a thin film having large microcrystallites. If the deposition takes place in special conditions, the films can be deposited in the form

of a conglomerate of nanoparticles. Then, due to a quantum size effect, the "optical gap" of these nanocrystallites increases drastically and therefore the photosensitivity range of this material is also extended.

This complex structure based on PbS nanocrystallites presents very interesting peculiarities. In order to understand the device characteristics we began our studies with a comparative investigation of the photoelectrical properties of the micro- and nano-crystallites layers itself. For this purpose we deposited the respective layers on a glass substrate and investigated their structural, optical and electrical properties, the thermally stimulated currents and their photoconductivity. The results will be reported in the first part of the paper. Then we will compare the electrical and optical characteristics of the $PbS/SiO_2/Si$ devices based on microcrystallite and nanocrystallite PbS. A field effect modulation of photoelectrical properties will be further reported. Finally we will analyze the effect of interface states and leakage currents on the C–V and photoelectrical characteristics.

This type of heterostructure has an important potential for applications as a new interesting type of optoelectronic device.

2. Experimental

The PbS films were deposited on glass or Si/SiO_2 substrates by a chemical bath deposition method.

The reaction for obtaining the PbS thin films is: $Pb^{2+} + S^{2-} \rightarrow PbS$.

The Pb^{2+} ions are obtained from a 0.06M $PbNO_3$ solution and will be precipitated by the S^{2-} ions from the 0.24M SC $(NH_2)_2$ solution. All details concerning film preparation are explained somewhere else [4]. The microcrystalline PbS thin film was deposited from a chemical bath containing reducing agent and Bi ions as doping element in about an hour. The nanocrystalline thin film was obtained after a shorter reaction time of about 17 minutes from the reducing bath without doping elements.

The substrates used for the deposition of the PbS thin film were high quality glass or p-Si (100) / SiO_2 with a Si resistivity of 31–46 Ω·cm and a thickness of about 180 nm of SiO_2, corresponding to a capacitance of about 300 pF for our dots area. The ohmic contacts were made with Al on Si and with Au on PbS. The area of the Au contact dots is 1.5 mm^2.

In this paper, we study PbS composite structures for two deposition temperatures of the PbS thin film: 23°Cand 24°C, respectively. The results concerning the C–V, G–V and charge storage are very similar for both structures, so results for the films deposited at 24°C will be preponderantly shown here.

The small signal C–V and G–V characteristics were measured using an Agilent bridge and the I–V curves under dark conditions were obtained using a Keithley dc source and an electrometer.

The photoelectrical measurements were performed in chopped light by using an Oriel monochromator, a lock-in amplifier and an incandescent lamp as a light source. The photoconductive signal is collected from a load resistance R_L.

3. Results

3.1. Electrical and photoconductive properties of PbS films deposited on glass

The average grain size of the microcrystallite PbS thin film optimized for high photosensitivity determined from the SEM pictures was found to be 250–300 nm, while for the nanocrystalline PbS film about 50 nm [4]. However, we found from optical measurements that the average size of the nanocrystallite films could be smaller than 3 nm. We concluded therefore that the distribution of crystallite dimensions is not uniform. The crystallite size is smaller near the substrate and larger at the surface.

Table 1 summarizes the properties of the PbS thin films deposited on glass substrates, under similar conditions as those used for deposition on p-Si/SiO_2.

Table 1. Properties of PbS thin films deposited on glass substrates

Dep. temp. [°C] -sample-	Dep.time [min]	Layer thickness [nm]	Sheet resistance [Ω/□]
24°C (A)	17 (Bi)	270	10^5 – 10^6
24°C (B)	17	270	5×10^7– 5×10^8
22°C (C)	17	90	2×10^{10}

In p-PbS microcrystalline films the hole concentration is relatively large (10^{17} cm^{-3}) [5] but the sheet resistance is not small, as we can observe in Table 1 (sample A), because of the small carrier mobility determined by the inter-grain barriers.

Table 1 shows a strongly increased sheet resistance of the nanocrystalline PbS B film, compared with a standard microcrystalline (film A) having the same thickness. This suggests a drastic reduction of the carrier concentration or of the mobility in these samples.

The large sheet resistance together with the presence of some sensitising centres, obtained as a consequence of some oxidizing treatments, allow for good photoconductive properties of these layers [5].

There is an optimum oxidizing temperature for good photoconductive properties and the best results were obtained for an oxidizing treatment made at 80°C for our case.

Our Thermally Stimulated Conductivity (TSC) measurements indicate also the presence of more deep traps in films treated at 400°C than in that treated at 80°C.

The spectral dependence of micro-film photoconductivity is characterised by an adsorption edge of about 3 000 nm (the bulb glass cuts the infrared radiation with wavelengths longer than about 2 700 nm), corresponding to the PbS crystalline energy gap, and a maximum at about 2 250 nm (Fig. 1a). A dramatic change is observed in the spectra corresponding to nanocrystalline films (Fig. 1b). Now the adsorption edge is displaced at about 2 500 nm and the maximum is situated at about 750–800 nm. We can suppose that the increase of the photocurrent in the short wavelength part is determined mainly by the photon absorption in the crystallites having small mean sizes. It is well known that the "optical gap" in nanocrystalls increases due to a quantum size effect and is connected with their dimensions R by the relation [6]:

$$E_g = \frac{\hbar^2\pi^2}{2R^2}\left(\frac{1}{m_e}+\frac{1}{m_h}\right) - \frac{1.786e^2}{\varepsilon R},$$

where m_e and m_h are the effective masses of electrons and holes respectively, ε is the dielectric constant and R is the size of the nanocrystal. In the absence of data concerning the values of these parameters we took those corresponding to the crystalline materials, i.e. $m_e = m_h \approx m_o$ and $\varepsilon = 170$. Then the calculated energy gap for different crystallite sizes are presented in Table 2.

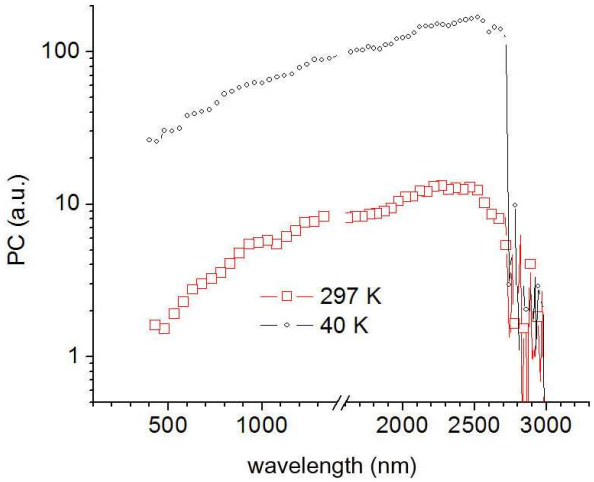

Fig. 1 (a). Photocurrent spectra for sample A.

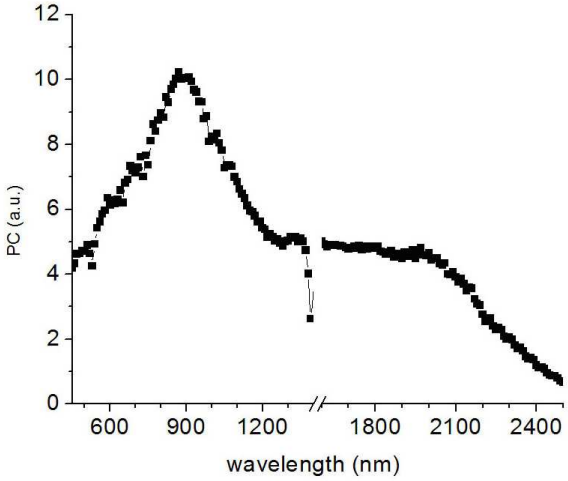

Fig. 1 (b). Photocurrent spectrum for sample B.

We observe in Fig. 1 that the important increase in the high energy part of the spectrum is situated around 1.4 eV that corresponds in Table 2 to a very small particle sizes of the order of 3.8 nm.

Table 2. Value of energy gap corresponding to different nanocrystallite sizes

Energy gap [eV]	Crystallite size R [nm]
1.25	4
1.4	3.8
2	2.7
2.8	2

3.2. PbS/SiO_2/Si heterostructures

This structure, together with the biasing schema for determination of the transversal I–V characteristics, is presented in Fig. 2.

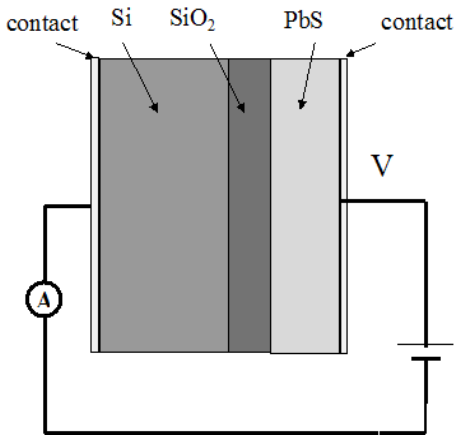

Fig. 2. Heterostructure Si/SiO_2/PbS under transversal bias conditions.

These characteristics are shown in Fig. 3 for both microcrystalline based PbS sample and that one based on nanocrystalline PbS. Both have asymmetrical leakage currents. For positive bias applied on the PbS thin film (p-type) the leakage current is large, increasing with bias. This increase is not entirely exponential, as for the case of an ideal diode, but quadratic for larger bias ($I \approx V^2$), as observed in the inset of Fig. 3. This dependence suggests a space charge limited transport mechanism, determined by the injection of carriers in the oxide region. For the above mentioned biasing the carrier injection takes place from the semiconductor PbS into the dielectric, mediated by 'impurity' channels in the oxide and by defects at the interface between the PbS semiconductor film and the SiO_2 dielectric [7]. The asymmetrical I–V characteristics

suggest however the presence of some barriers that control the carrier injection. Considering that injection takes place only after the deposition of PbS and that PbS films are p-type, it is reasonable to assume that the injected carriers are holes from PbS.

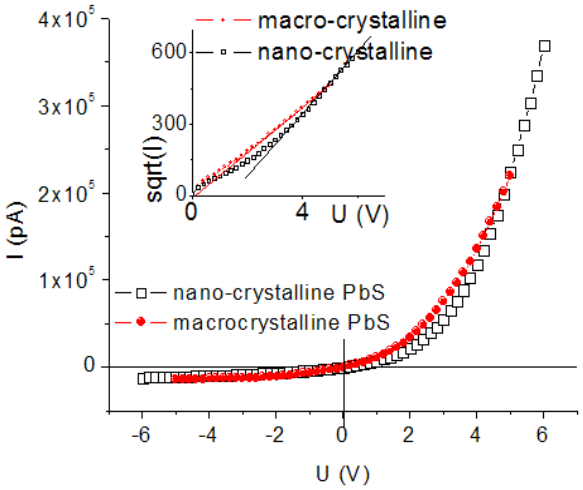

Fig. 3. Transversal I–V curves
for the heterostructures in Fig. 2.

Figs. 4 (a) and (b) show the C–V and G–V characteristics of a sample having microcrystalline PbS layer, under dark conditions. It can be observed a hysterezis effect which is significant only at high frequency.

More interesting are the C–V and G–V characteristics for the nanocrystallite based heterostructures presented in Fig 5. In this case the hysterezis effect is seen at all frequencies with about the same loop area. This area increases if the sweeping voltage increases (graph not shown). Except this hysterezis effect, the general aspect of these C–V curves is similar to that of an ideal MOS structure. However, some peculiarities are present. Thus, at low frequency a dramatic increase of the capacitance takes place. This is true also for the microfilms. Please, note that the y scale (capacitance) in this case (Fig. 4) is logarithmic while the corresponding scale in Fig. 5 is linear.

An other strange aspect is the fact that for the frequency of 100 Hz, the capacitance increases above the oxide capacitance for positive bias. In accumulation, the flat capacitance decreases if the frequency increases. We observe also that the flatband voltage for the nanocrystalline based structures is displaced on the right comparatively with the microcrystalline structures.

For sample B, we also observe that the hysterezis shape does not change significantly by reversing the direction of the sweeping voltage. Both the C–V and the G–V characteristics are similar when sweeping the voltage from –10 V to +10 V compared to a sweep direction from +10 V to –10 V. By integrating the C–V curves we obtain a

stored charge density of about 1.1×10^{11} cm^{-2} for a sweep voltage range from –5 V to +5 V and 3×10^{11} cm^{-2} for a sweep voltage range from –10 V to +10 V, respectively.

Table 2.

Measurement frequency	Stored charge/cm^2		
	Micro-PbS	Nano-PbS +10V:–10V	Nano-PbS +5V:–5V
100 kHz	1.3×10^{11}	2.7×10^{11}	1.1×10^{11}
10 kHz	2.6×10^{11}	2.9×10^{11}	1.2×10^{11}
1 kHz	–	3.1×10^{11}	1.2×10^{11}
100 Hz	–	5×10^{11}	1.1×10^{11}

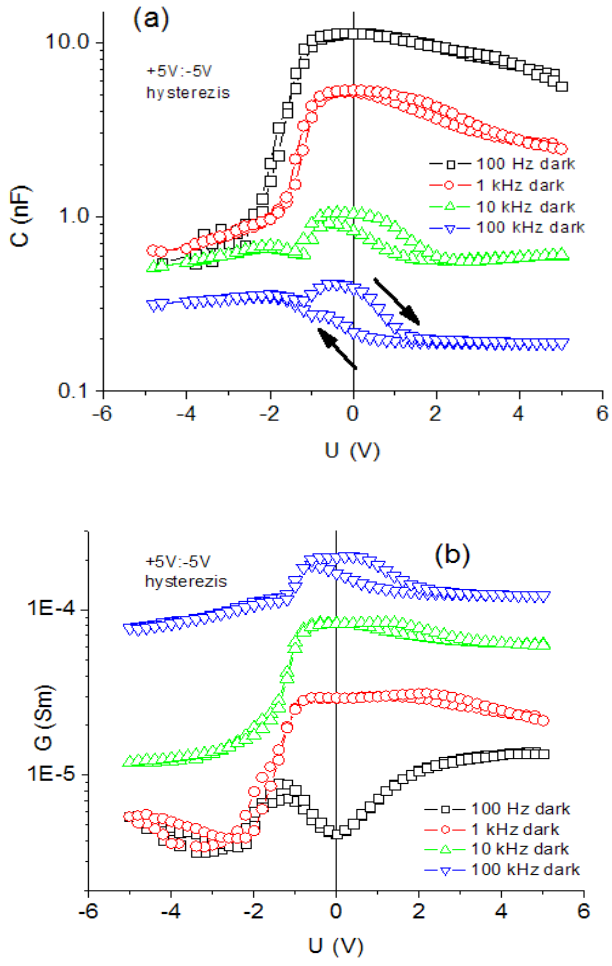

Fig. 4. Dark C–V and G–V characteristics for a sample with macrocrystalline PbS.

Table 2 shows the stored charge per unit area deduced by integration of the C–V curves for the microcrystalline PbS based structures and for the nanocrystalline PbS ones, for two different sweeping voltage ranges, +5V: –5 V and +10 V: –10 V, respectively. The total measurement time is the same in both cases $t = 830$ s. From Table 2 it can be observed that the stored charge for the nano-sample depends on the maximum sweeping voltage, being a factor of about two larger for 10 V than for 5 V.

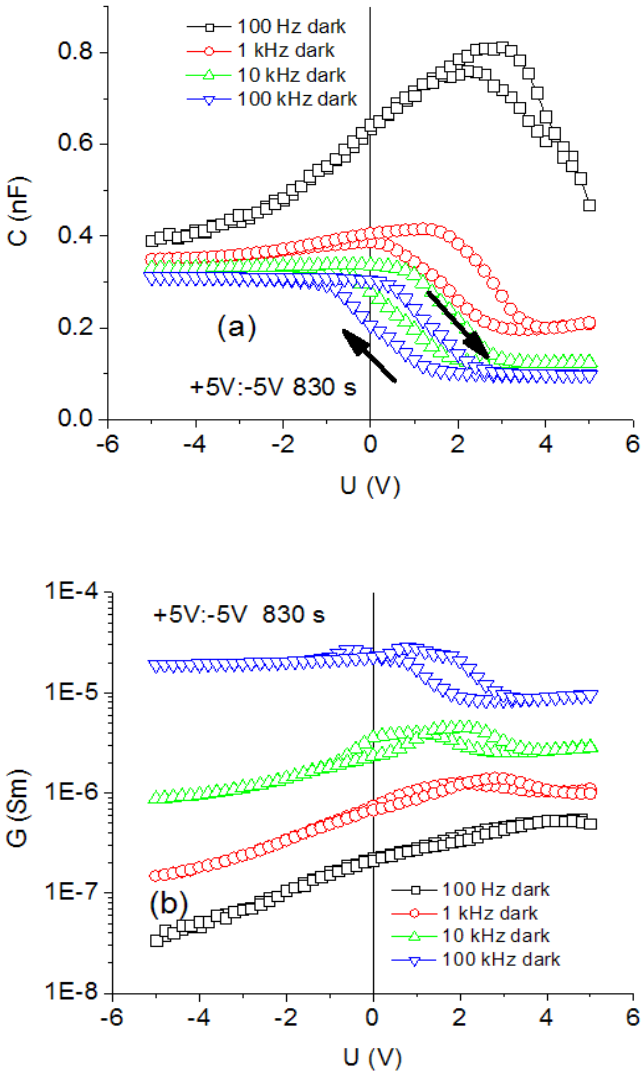

Fig. 5. Dark C–V and G–V characteristics for a sample with nanocrystalline PbS.

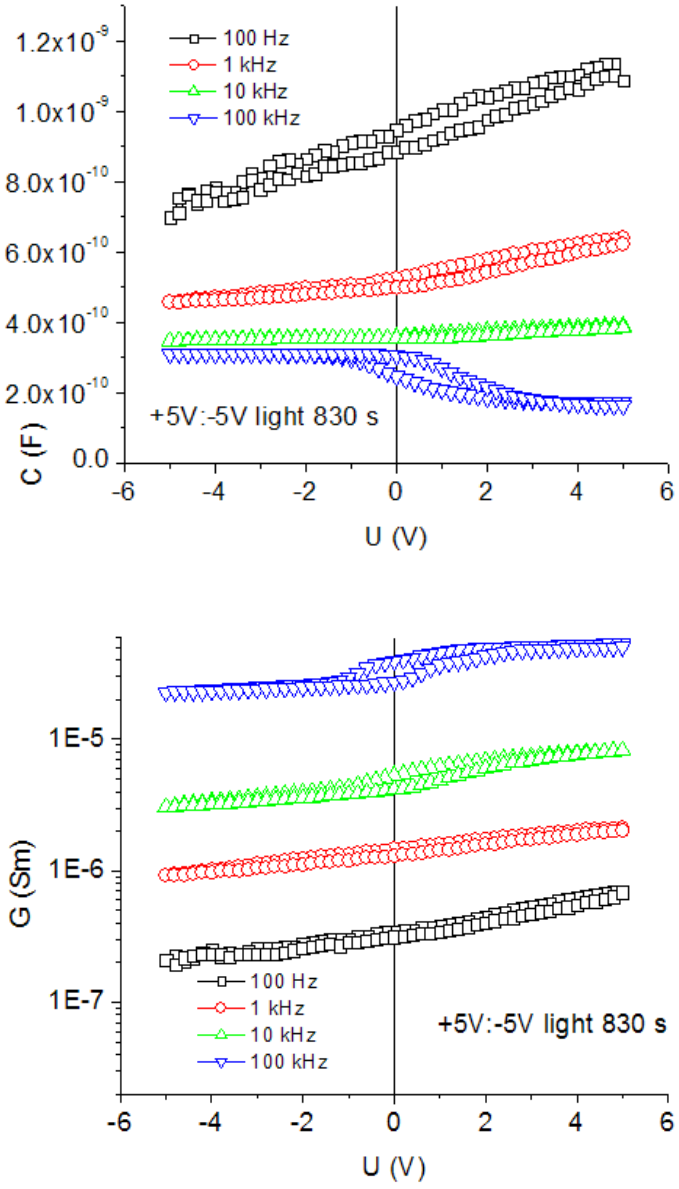

Fig. 6. C–V and G–V characteristics for a sample with nanocrystalline PbS with sample illumination.

The sample illumination has an important effect on both C–V and G–V characteristics. As we can see in Fig. 6 the hysterezis loop areas are reduced drastically by illumination.

3.3. Field assisted effects

The structure for field effect measurements together with the biasing scheme is shown in Fig. 7. The voltage dependence of the Source-Drain (S-D) current is linear for microcrystalline based structures (graph not shown). However, in the case of nanocrystalline samples the dark I–V characteristics are asymmetric and the S-D currents depends on the gate voltage and polarity (Fig. 8).

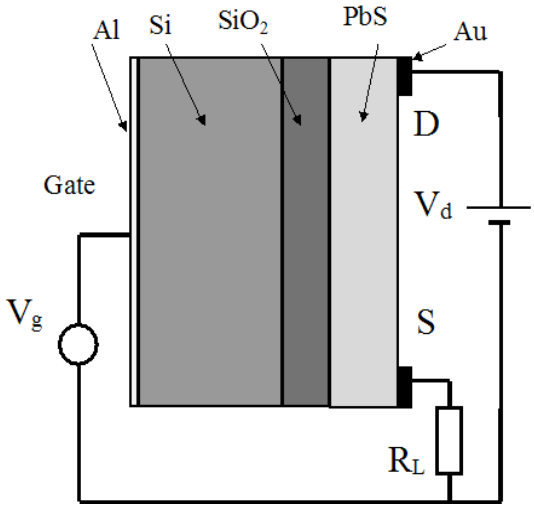

Fig. 7. Biasing scheme for field-effect measurements.

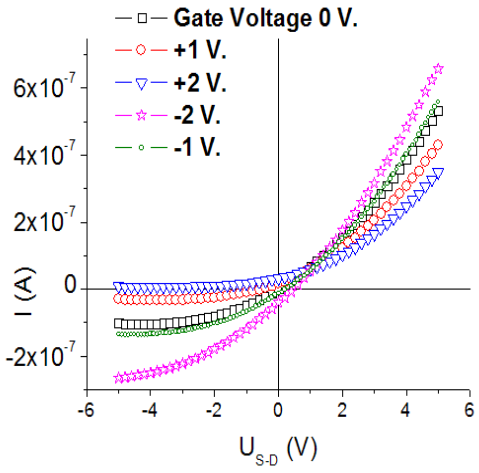

Fig. 8. Dark I–V characteristics S-D having the gate voltage as a parameter.

Thus, if the Si gate has a negative polarity the S-D current increases in both directions. Inverting the gate voltage, the S-D currents are now reduced and at a higher gate negative voltage even change their direction. An important effect of gate biasing can be observed also on the spectral S-D photoconductivity characteristics (Fig. 9).

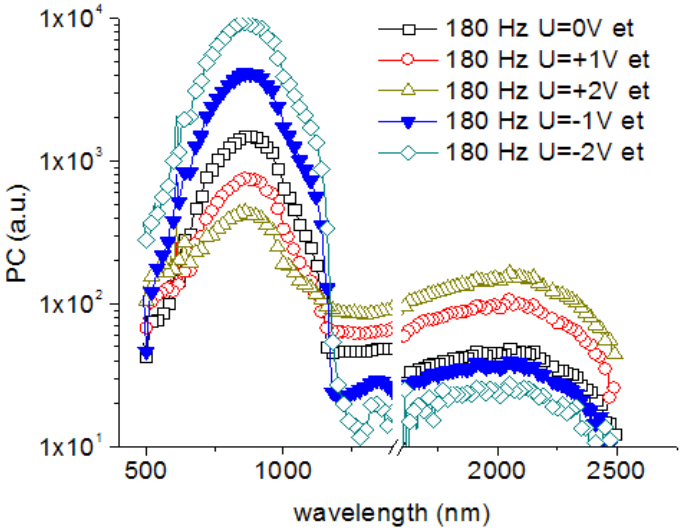

Fig. 9. Photocurrent spectrum for sample B with the gate voltage as a parameter.

Thus, for negative polarity on the "Si gate" the short wavelength maximum increases drastically and the long wave photocurrent is reduced. For positive gate polarity the reverse is true. We outline that the abrupt increase of the short wavelength maximum at 1.1 eV corresponds to the Si energy gap. This fact suggests that the photocurrent is determined mainly by the carriers created in Silicon.

3.4. Analysis

The investigated PbS/SiO_2/Si structure represents a Metal-Semiconductor-Insulator-Semiconductor-Metal (MSISM) system. It is difficult to draw an energy band diagram for this structure, especially for the case involving nano-PbS. This happens because there is a lack of data concerning the affinity and work function of this nonhomogeneous material. We have also no information about the complex interfaces involved in this structure. Therefore in the following we will made only qualitative considerations.

We will start our analysis extracting some information from the experimental data presented above. Thus, the high sheet resistance of nano-PbS indicates a low carrier concentration and/or low mobility. The carrier concentration in the p-type Silicon is

about 5×10^{14} cm^{-3}, significantly smaller than that in the PbS microcrystalline grains. If the reverse is true for nanocrystalline grains situated near the interface, it would be expected that the space charge is extended in the whole PbS region. However we have no evidence that this happens.

As observed above, the C–V curves of the nano-structures are shifted to the right if we compare them with those of micro-structures. This fact suggest that a high concentration of negative charge is trapped at the interfaces. This negative charge could bring both semiconductor regions in a hole accumulation state. If the sweep voltage goes towards positive values, the Silicon interface region is exhausted from holes, the space charge region is extended and the total capacitance decreases as this happens in usual MOS structures. In the same time the PbS region is in accumulation and the entire capacitance is determined by that of Si. If the positive voltage increases further an important hole injection from the PbS side into the Silicon side takes place through the leakage channels as we observe in Fig. 3. Then, the holes in excess will recombine with trapped electrons or are trapped on other levels, reducing in this way the net negative charge. In the sweeping process towards negative voltages the entire C–V characteristic will be shifted to the left if the hole emission into the valence band takes place with a long time constant. This explains the hysterezis behavior of the C–V curves. This mechanism involves, as we said, a relative long time constant for reaching each equilibrium state. Increasing the sweeping range and thus the measuring time, the negative charge on the traps decreases further and thus the C–V curve is shifted more on the left, increasing in this manner the loop area. If the voltage on PbS is negative, the depleted region is now in PbS. However, due to its high dielectric constant and small thickness its capacitance can never be lower than the oxide capacitance, which controls the value of the total capacitance in this voltage range.

The illumination creates electron hole pairs. The capture of holes reduces the net negative charge and thus the hysterezis effect is strongly reduced (Fig. 6).

The C–V curves shift with frequency, a phenomenon which is found also in other heterostructures, was explained by the presence of traps that exchange carriers with the main band and can respond, in the investigated frequency range, to the ac signal [7]. This happens, probably, also in our structures.

The flat accumulation capacitance decrease with the increase of frequency is the effect of a series resistance which is expectable to be present in our structures due to the high sheet resistance of neutral zones [8].

Another interesting phenomenon is the important increase of the low frequency capacitance above the insulator capacity. The fact that this happens only at low frequency suggests that only some traps which are present in the PbS or oxide regions and have long time constant are involved.

The G–V plots show a strong frequency dispersion of the conductivity for nano-structures varying as a power of frequency. This behavior is characteristic to disordered solids, either due to defects in the oxide layer or due to the poly (nano) crystalline nature of the PbS film.

The interesting phenomena related to the field effects presented in the previous section are connected with the nano-structure peculiarities mentioned above. Thus,

for negative Si biasing (positive on PbS) the space charge region in PbS decreases and a hole channel near the interface appears eventually. Then the source is connected to the drain by this channel. If the negative voltage increases, the channel is extended, its resistance is reduced and the S-D current increases. This effect can indeed be observed in Fig. 8. For positive Si bias the channel is narrowed. Therefore the S-D current is reduced in both directions (Fig. 8). At larger positive gate voltages the S-D current can be so low that the leakage current due to the injection of holes from the Si side is larger than the current flowing directly from the source to the drain and have opposite direction. This happens indeed in our structures (Fig. 8).

The gate voltage dependence of the photoconductivity spectral characteristics (Fig. 9) has the same explanation. If the "Si gate" is under negative bias, the space region is large in Si and narrow in PbS. Thus more carriers are collected in Si and fewer in PbS than without gate biasing. Then, due to communication between the two regions via leakage channels, the photocurrent increases in the short wavelength range corresponding to a preponderantly absorption of light in the Si region and decreases in the long wavelength range corresponding to the absorption of light on larger PbS grains. For positive gate biasing the reverse is true (Fig. 9).

4. Conclusions

The comparative analysis made above showed that the PbS/SiO2/ Si heterostructures based on nanostructured PbS have some peculiarities that open the possibility for new applications. Using a field effect structure it is possible to control the short to long wavelength ratio. Also the photoelectrical sensitivity of this structure could be enhanced by this field effect control.

A nice hysterezis effect in C–V and G–V characteristics was found in nanocrystalline based heterostructures. This and other interesting phenomena related to this kind of heterostructures were explained by taking into account the effect of the interface trapped carriers and of the leakage currents on their electrical and photoelectrical properties.

Acknowledgements. This work was supported by the Romanian Ministry of Education and Research in the frame of grant CNCSIS no. GR124.

References

[1] STECKL, A.J., ELABD, H., TAM, K.-Y., SHEU, S.-P., MOTAMEDI, M.E., *The optical and detector properties of the PbS-Si heterojunction*, *IEEE Trans. Electr. Dev.*, vol. **ED-27**, pp. 126–133, 1980.

[2] FENG, T., YU, H., DICKEN, M., HEATH, J. R., ATWATER, H. A., *Probing the size and density of silicon nanocrystals in nanocrystal memory device applications*, Appl. Phys. Lett., vol. **86**, pp. 0331031-3, 2005.

[3] LIU, Z., LEE, C., NARAYANAN, V., PEI, G., KAN, E. C., *Metal nanocrystal memories – Part I: Device design and fabrication*, *IEEE Trans. Electr. Dev.*, vol. **49**, no. 9, pp. 1606–1613, 2002.

[4] E. PENTIA, L. PINTILIE, I. MATEI, T. BOTILA, E. OZBAY, *Chemically prepared nanocrystalline PbS thin films*, Journ. Optoelectronics and Advanced Materials, vol. **3**, no. 2, pp. 525–530, 2001.

[5] S. ESPEVIK, C.-H. WU, R.H. BUBE, *Mechanism of photoconductivity in chemically deposited lead sulfide layers*, J. Appl. Phys., vol. **42**, no. 9, pp. 3513–3529.

[6] Y. WANG, N, HERRON, *Nanometer-sized semiconductor clusters: materials synthesis, quantum size effects and photoelectrical properties*, J. Phys. Chem., vol. **95**, pp. 525–532, 1991.

[7] GOLDENBLUM, A., PINTILIE, I., BUDA, M., POPA, A., LISCA, M., BOTILA, T., TEODEORESCU, V., *Electrical properties of as-grown MBE high-k gate dielectrics deposited on silicon*, J. Appl. Phys., vol. **99**, pp. 064105 1–9, 2006.

[8] NICOLLIAN, E.H., BREWS, J.R., *MOS (Metal Oxide Semiconductor) Physics and Technology*, John Wiley & Sons, New York, 1982.